Science Advances

AAAS

advances.sciencemag.org/cgi/content/full/4/2/eaar2177/DC1

Supplementary Materials for

Direct single-molecule dynamic detection of chemical reactions

Jianxin Guan, Chuancheng Jia, Yanwei Li, Zitong Liu, Jinying Wang, Zhongyue Yang, Chunhui Gu, Dingkai Su, Kendall N. Houk, Deqing Zhang, Xuefeng Guo

Published 9 February 2018, *Sci. Adv.* **4**, eaar2177 (2018)
DOI: 10.1126/sciadv.aar2177

This PDF file includes:

- Supplementary Materials and Methods
- scheme S1. Synthetic routes to the carbonyl molecule (compound **4**) with a 9-fluorenone functional center and $-NH_2$-terminal groups.
- fig. S1. Schematic of fabricating graphene FET arrays.
- fig. S2. Schematic of fabricating graphene point contact arrays.
- fig. S3. Electrical measurements of single-molecule junctions.
- fig. S4. *I-t* curves and corresponding histograms of current values for a typical GMG-SMJ in different environments at 298 K.
- fig. S5. Representative *I-V* and d*I*/d*V*-*V* curves of a control device.
- fig. S6. *I-t* curves and corresponding histograms of current values for a control device in different environments at 298 K.
- fig. S7. MPSH spectra of the molecule in the RS and IS.
- fig. S8. LC-MS characterizations of the two-step reaction.
- fig. S9. Plots of time intervals.
- fig. S10. Additional solvent-dependent experiments.
- Reference (*40*)

Supplementary Materials and Methods

1. Molecular synthesis

The reagents and starting materials including compound **3** were commercially available, which were used without any further purification if not specified elsewhere. Compound **1** was synthesized by following the reported procedures (*40*).

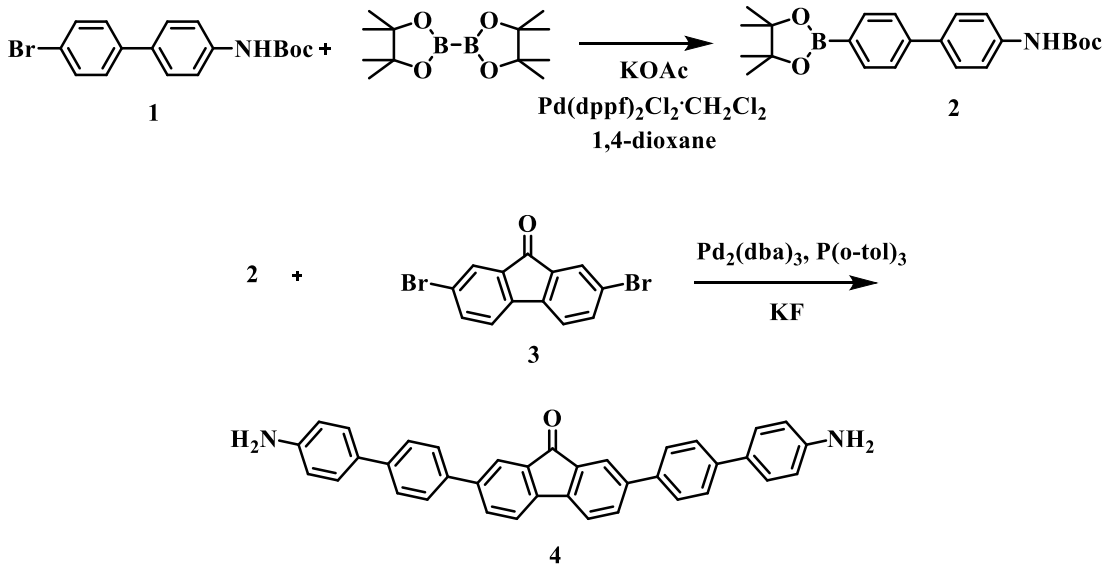

scheme S1. Synthetic routes to the carbonyl molecule (compound 4) with a 9-fluorenone functional center and −NH_2-terminal groups.

1.1 Synthesis of compound 2

Compound **1** (6.4 mmol, 2.21 g), 4,4,4′,4′,5,5,5′,5′-octamethyl-2,2′-bi (1,3,2-dioxaborolane) (31.6 mmol, 3.10 g), KOAc (4.80 g), and a catalytic amount of [1,1′- bis-(diphenylphosphino)ferrocene]palladium(II) chloride ($Pd(dppf)_2Cl_2·CH_2Cl_2$) (0.6 mmol, 0.50 g) were dissolved in 30 mL of anhydrous 1,4-dioxane. The reaction mixture was then heated at 80 °C and stirred overnight under N_2. After cooling down to room temperature, the solvent was removed under reduced pressure. The crude product was purified by column chromatography with petroleum ether (60–90 °C) and CH_2Cl_2 (1:2, v/v) as the eluent. Compound **2** was obtained as white solids (2.3 g, 91.8%). ^{1}H NMR ($CDCl_3$, 400 MHz): δ 7.86 (d, 2H, J = 8.0 Hz), 7.58–7.55 (m, 4H), 7.43 (d, 2H, J = 8.4 Hz), 6.53 (s, 1H), 1.54 (s, 9H), 1.36 (s, 12H). HRMS (EI) m/z:

[M]+ calcd for $C_{23}H_{30}BNO_4$, 395.2268; found, 395.2261.

1.2 Synthesis of Compound 4

Compounds **2** (316.2 mg, 0.8 mmol) and **3** (67.6 mg, 0.2 mmol) were dissolved in the mixture of toluene (20 mL) and water (5 mL). The solution was purged with N_2 for 10 min, followed by addition of $Pd_2(dba)_3$ (9.2 mg, 0.01 mmol), PPh_3 (21 mg, 0.08 mmol) and KF (150.6 mg, 1.6 mmol). The reaction mixture was stirred at 95 ^oC for 2 days. The product was precipitated out of the reaction. After cooling down to room temperature, the solvent was evaporated, and CH_2Cl_2 and petroleum ether (60–90 °C) were added to the mixture. By using centrifuge machine, the reaction mixture was collected. And they were washed with water, C_2H_5OH, ethyl acetate, acetone and CH_2Cl_2 for several times. Finally, compound **4** was obtained as grey solids (57.2 mg, 55.6 %). HRMS (TOF) m/z: [M]+ calcd for $C_{37}H_{26}N_2O$, 514.2045; found, 514.2045. Anal. Calcd for $C_{37}H_{26}N_2O$: C, 86.35; H, 5.09; N, 5.44. Found: C, 86.14; H, 5.17; N, 5.23.

1.3 Synthesis of [1,1':4',1":4",1"':4"',1"":4"",1"""-Sexiphenyl]-4,4"""-diamine

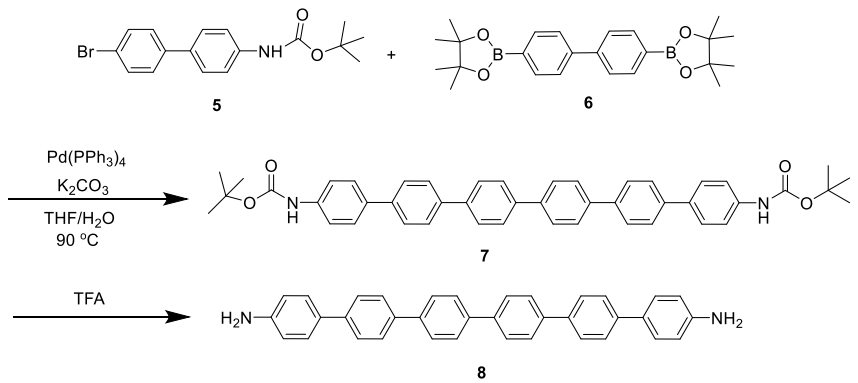

To a three-necked schlenk flask (150 mL) were added **5** (1.04 g, 3 mmol), **6** (0.41 g, 1 mmol), K_2CO_3 (1.80 g, 13.0 mmol), and $Pd(PPh_3)_4$ (58 mg, 0.05 mmol). The flask was evacuated and back-filled with argon atmosphere over three times, after which a degassed THF/H_2O co-solvent (15 mL/7 mL) was injected into the flask through syringe. The mixture was heated up to 90 °C and stirred for 14 h. After cooling down

to room temperature, the reaction mixture was poured into water , and then extracted with CH_2Cl_2. The organic layer was dried over anhydrous $MgSO_4$ and filtered off from an insoluble fraction. The solvent was removed under reduced pressure. Then the crude product was purified by silica gel column chromatography (eluent, petroleum ether: ethyl acetate = 9:1) to give compound **7** as a light-yellow powder. This solid was then dissolved in a mixture of CH_2Cl_2 (3 mL) and TFA (3 mL) and stirred for 2 h at room temperature. The solvent was removed under vacuum to give the target compound **8** (0.37g, 75%) as a light yellow powder. ^{1}H NMR (d_6-DMSO, 400 MHz, ppm) δ 7.99–7.60 (m, 16H), 7.47 (d, J = 7.4 Hz, 4H), 6.67 (d, J = 6.7 Hz, 4H), 5.28 (s,4H). HR-MS (MALDI-TOF, m/z): calcd. For $C_{36}H_{28}N_2$: 488.2252 [M^+]; Found: 488.2265.

2. Fabrication processes of single-molecule Junctions

2.1 Fabrication of graphene FET arrays

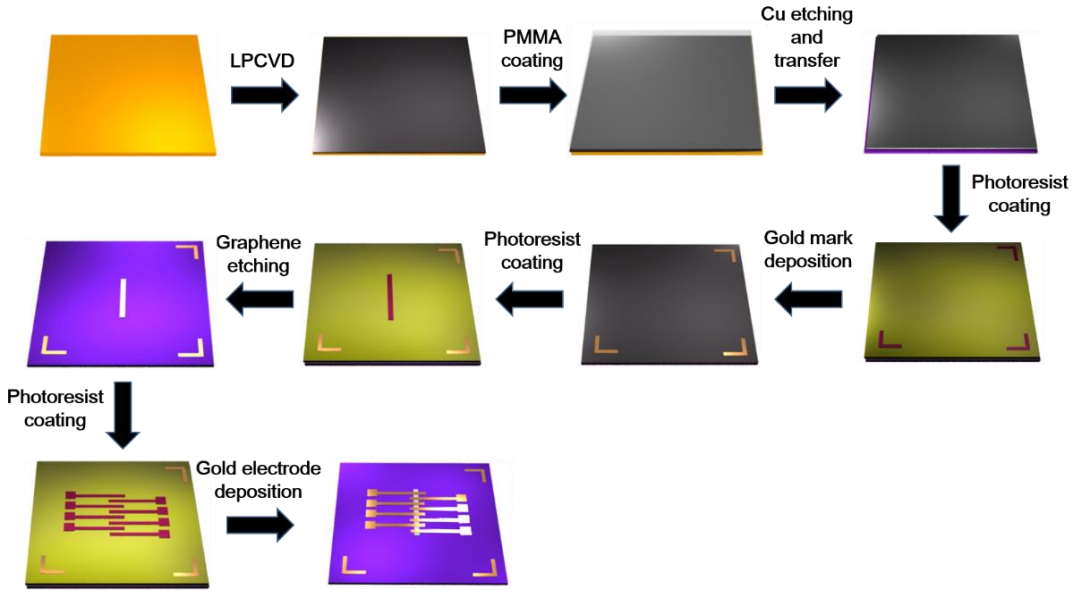

fig. S1. Schematic of fabricating graphene FET arrays. Single-layer graphene was grown on copper films via a LPCVD process, and was transferred onto Si wafers after spin-coating a layer of PMMA and etching the copper film. After three steps of photolithography, two steps of thermal evaporation and one step of oxygen plasma etching, graphene FET arrays were fabricated.

2.2 Fabrication of graphene point contact arrays

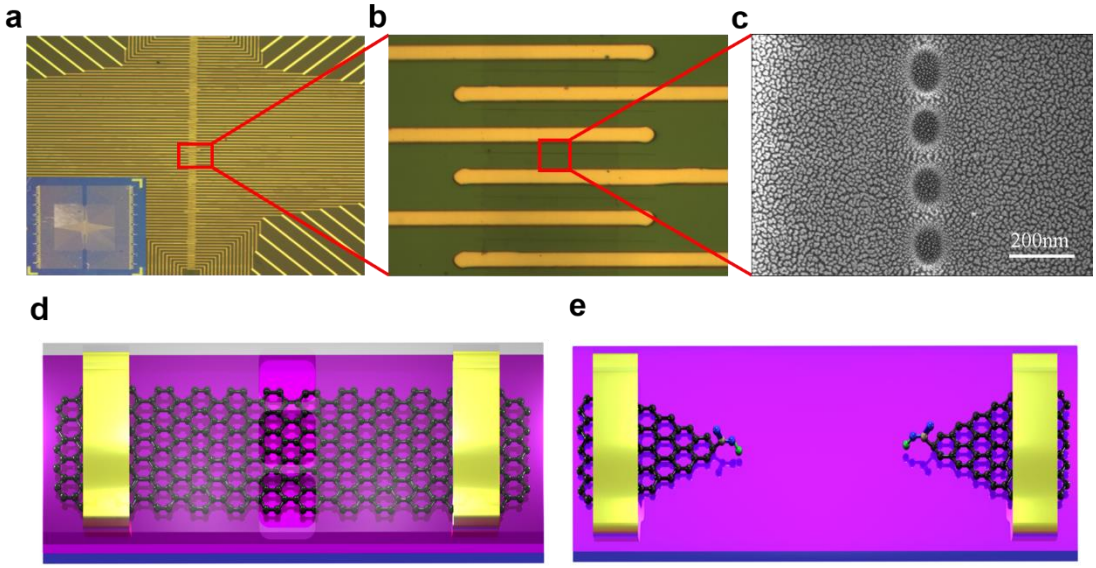

fig. S2. Schematic of fabricating graphene point contact arrays. (**a**,**b**) Optical microscopic images of graphene FET arrays with different magnifications. (**c**) SEM image of a dash-line mask fabricated by electron beam lithography (EBL). (**d**,**e**) Schematic representation of graphene nanoribbon processed by a dash-line lithographic method (d), and after precise oxygen etching, graphene point contact electrodes with carboxyl terminals were formed (e).

3. Analysis of single-molecule connection probability

Previously, a theoretical calculation has been done to prove single-molecule connection (*31*). Considering the probability of the molecular connection as G_n, where n is the number of rejoined junctions, then G_n can be given by the binomial distribution:

$$G_n = \frac{m!}{n!\,(m-n)!} p^n (1-p)^{m-n}$$

where m is the number of graphene point contact pairs (210 in the current case) and p the probability of successful connection for each junction.

When one or more than one molecule connects to the junction, the device will be

conductive, and therefore, the probability of successful connection $Y_{\text{connection}}$ should be:

$$Y_{\text{connection}} = 1 - G_0 = \frac{m!}{0!\,(m-0)!}p^0(1-p)^m = 1-(1-p)^m$$

On the basis of the experimental fact that ~20% junctions showed successful connection with an increased conductance, the ratio of single-junction devices is ~ 80%, illustrating that in most cases, charge transport in these devices mainly exists in a single-molecule junction.

4. Electrical measurements of single-molecule junctions

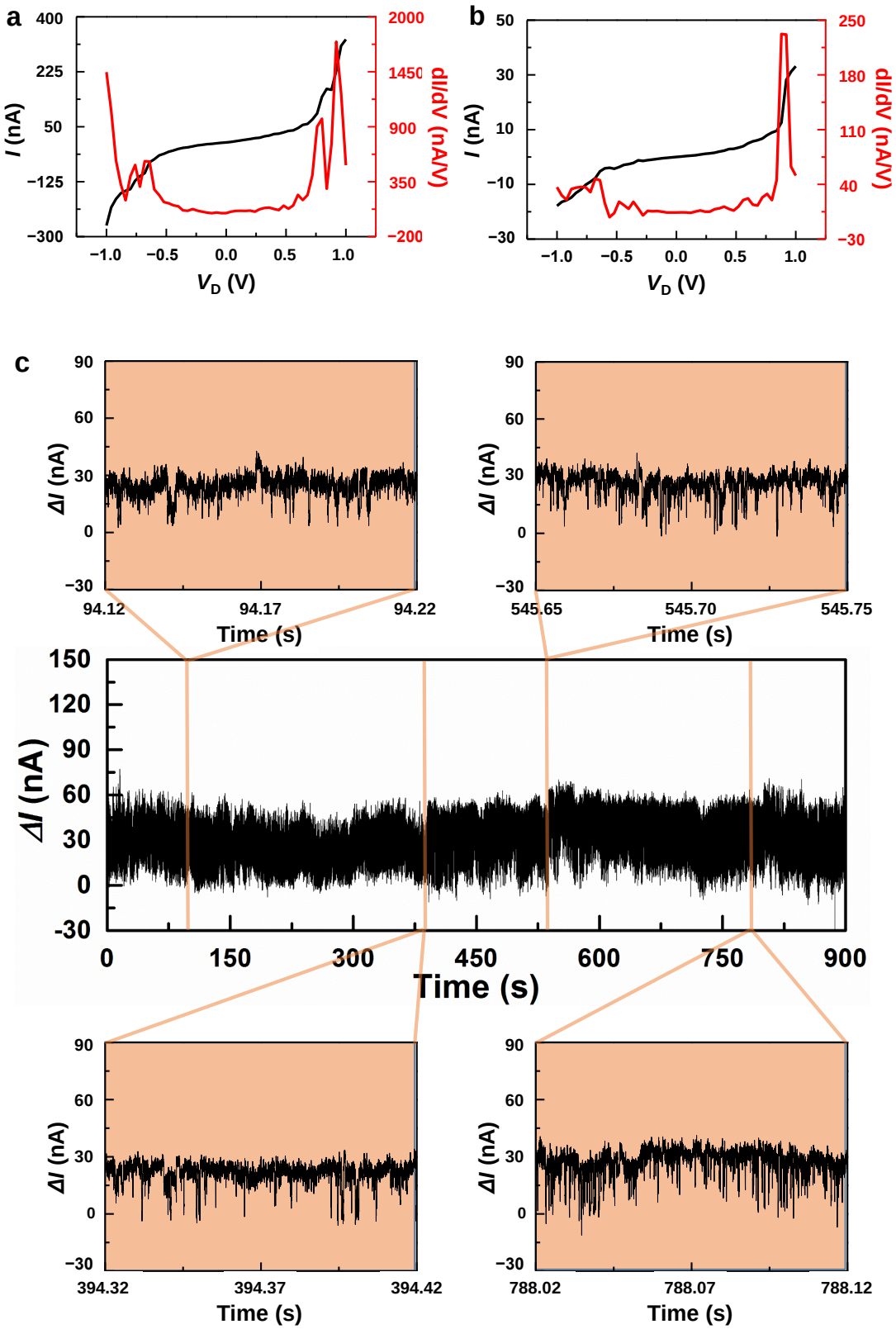

fig. S3. Electrical measurements of single-molecule junctions. (a,b) Representative

I-*V* and d*I*/d*V*-*V* curves of typical GMG-SMJs, proving the success of molecular immobilization. (c) Long-time *I*-*t* measurements of a different GMG-SMJ in the solution of ethanol at 298 K, which demonstrate the good device stability. V_D = 300 mV.

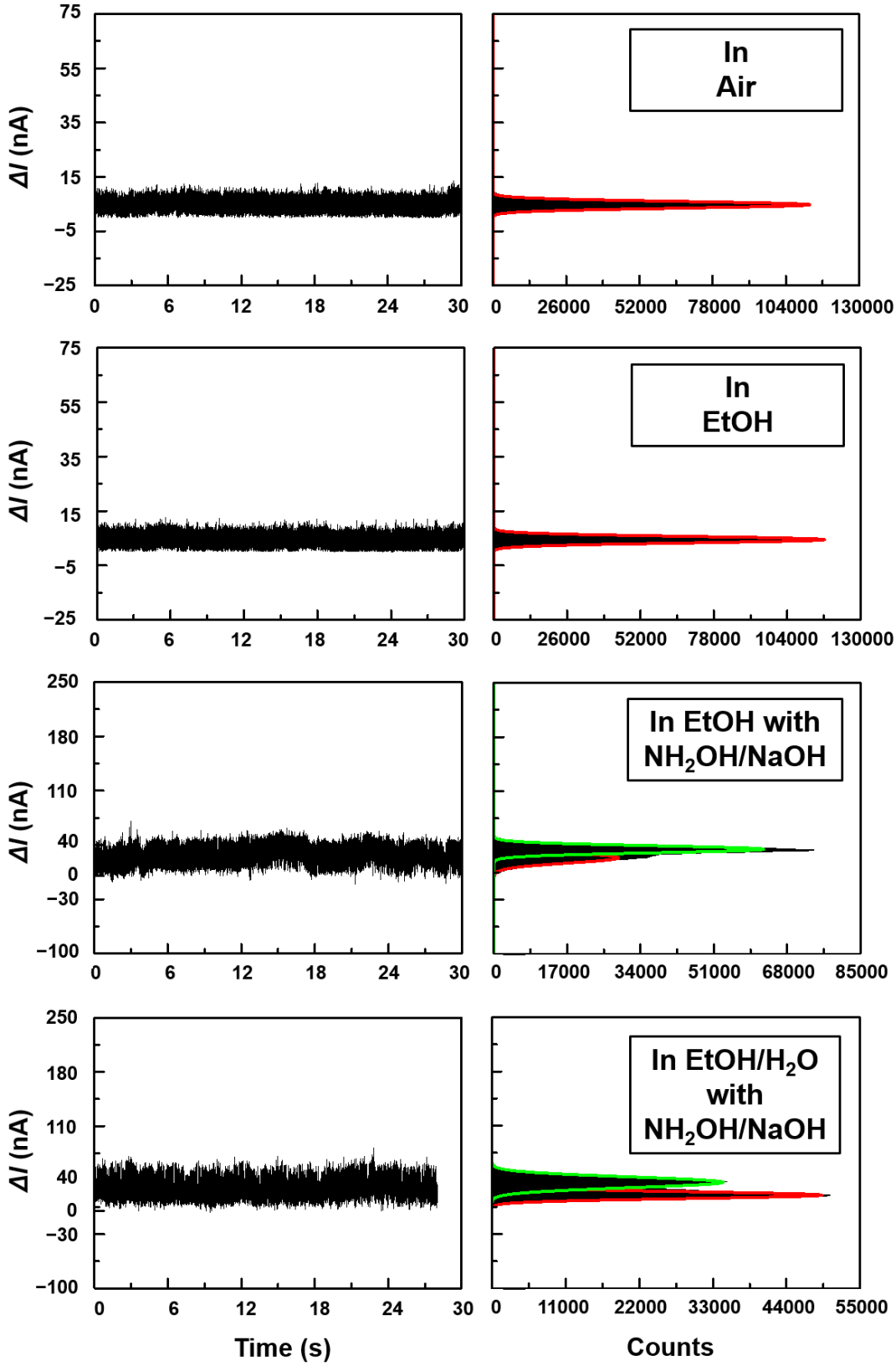

fig. S4. *I-t* curves and corresponding histograms of current values for a typical GMG-SMJ in different environments at 298 K. V_D = 300 mV.

5. Characterization of a Control Device

Control GMG-SMJs connected with a [1,1’:4’,1”:4”,1”’:4”’,1””:4””,1”””-Sexiphenyl]-4,4”””-diamine molecule (without the functional ketone center) were used and characterized under the same condition with working GMG-SMJs.

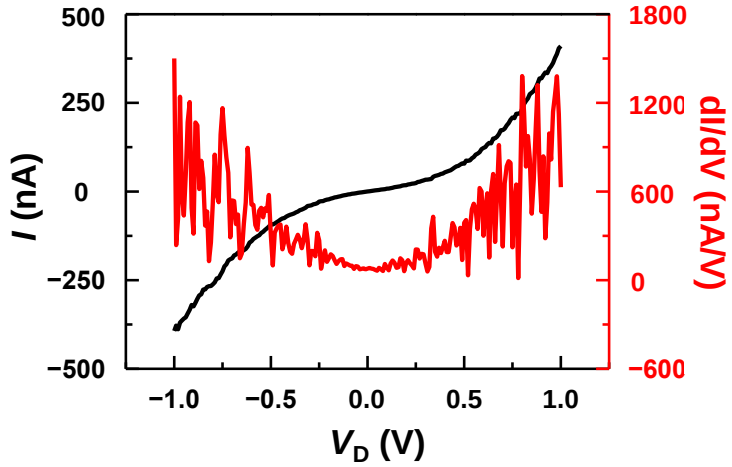

fig. S5. Representative *I*-*V* and d*I*/d*V*-*V* curves of a control device.

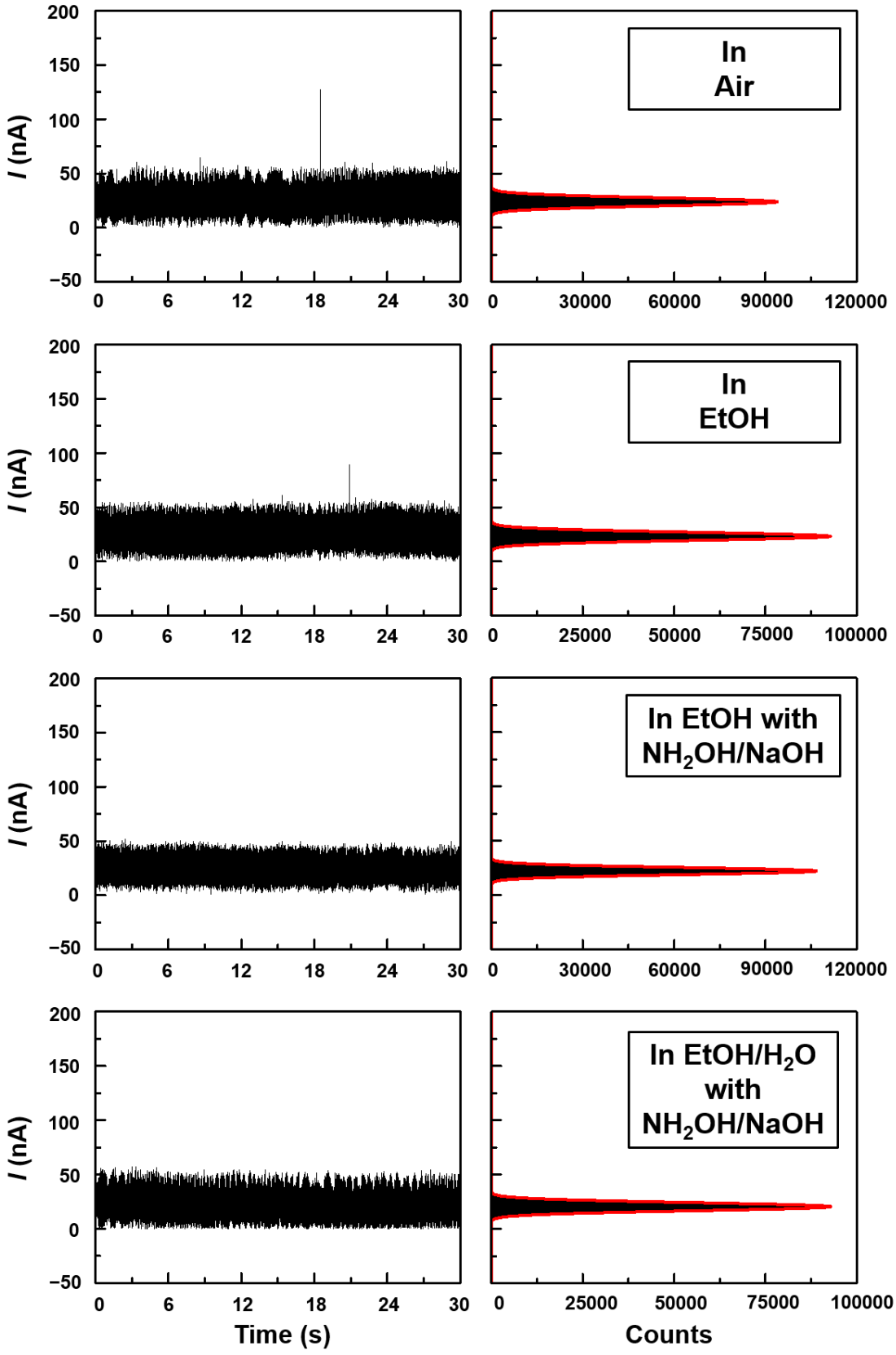

fig. S6. *I-t* curves and corresponding histograms of current values for a control device in different environments at 298 K. V_D = 300 mV.

6. Computational analyses

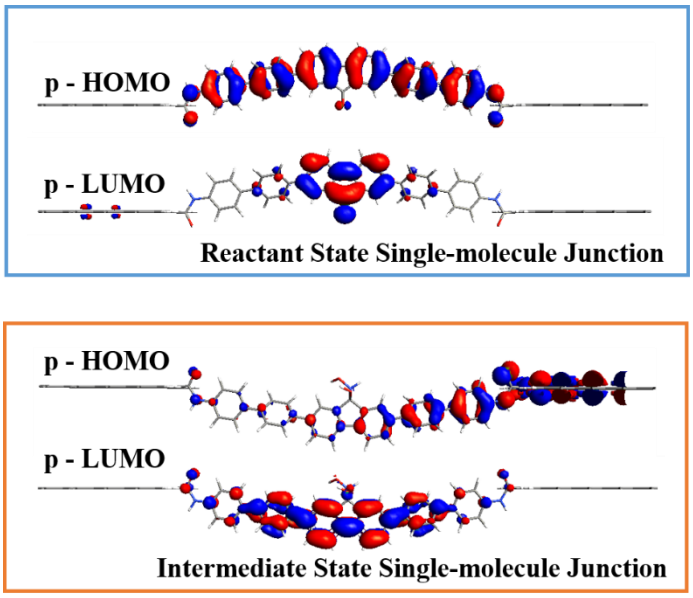

fig. S7. MPSH spectra of the molecule in the RS and IS. p-HOMO is more delocalized and acts as the major conductive tunnel for the reactant state and the reactant state has a better conductance.

7. LC-MS characterizations

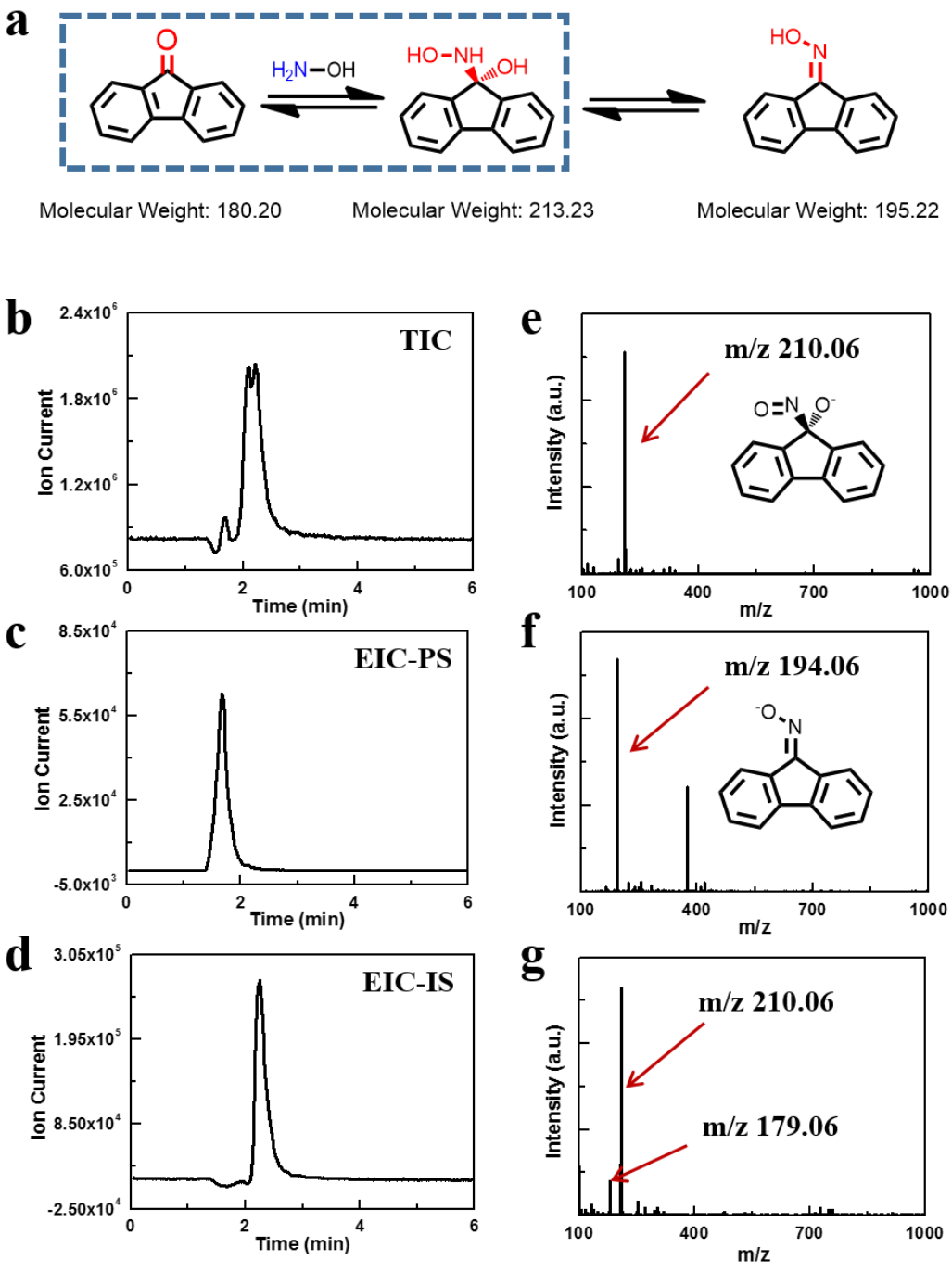

fig. S8. LC-MS characterizations of the two-step reaction. (**a**) The reaction process of 9-Fluorenone with NH_2OH, and the corresponding molecular weights of each state. (**b**) The total ion current (TIC) chromatogram of the reaction solution. (**c**,**d**) The extracted ion current (EIC) chromatogram of the production state (c) and intermediate state (d). (**e**) The mass spectrum (negative mode) of the mixed reaction solution. An

obvious MS peak of the intermediate state (M-3H, precursor ion m/z: 210.06) can be observed. (**f**) The mass spectrum (negative mode) of the product (M-H, precursor ion m/z: 194.06) eluted from chromatographic column. (**g**) The mass spectrum (negative mode) of the intermediate eluted from chromatographic column. The MS peaks for the intermediate state (M-3H, precursor ion m/z: 210.06) and the reactant state (M-1, precursor ion m/z: 179.06) illustrate the reverse reaction between the reactant and the intermediate.

8. Kinetic analyses of the single-molecule junction

I-t data in Figure 3 were analyzed by a segmental k-means method based on the hidden Markov model by using a QUB software (*30*). The fluctuation of the *I-t* signals was idealized and separated into two states. Further analysis provided one set of kinetic parameters, via a single-exponential fitting, including the lifetimes τ_{high} and τ_{low}.

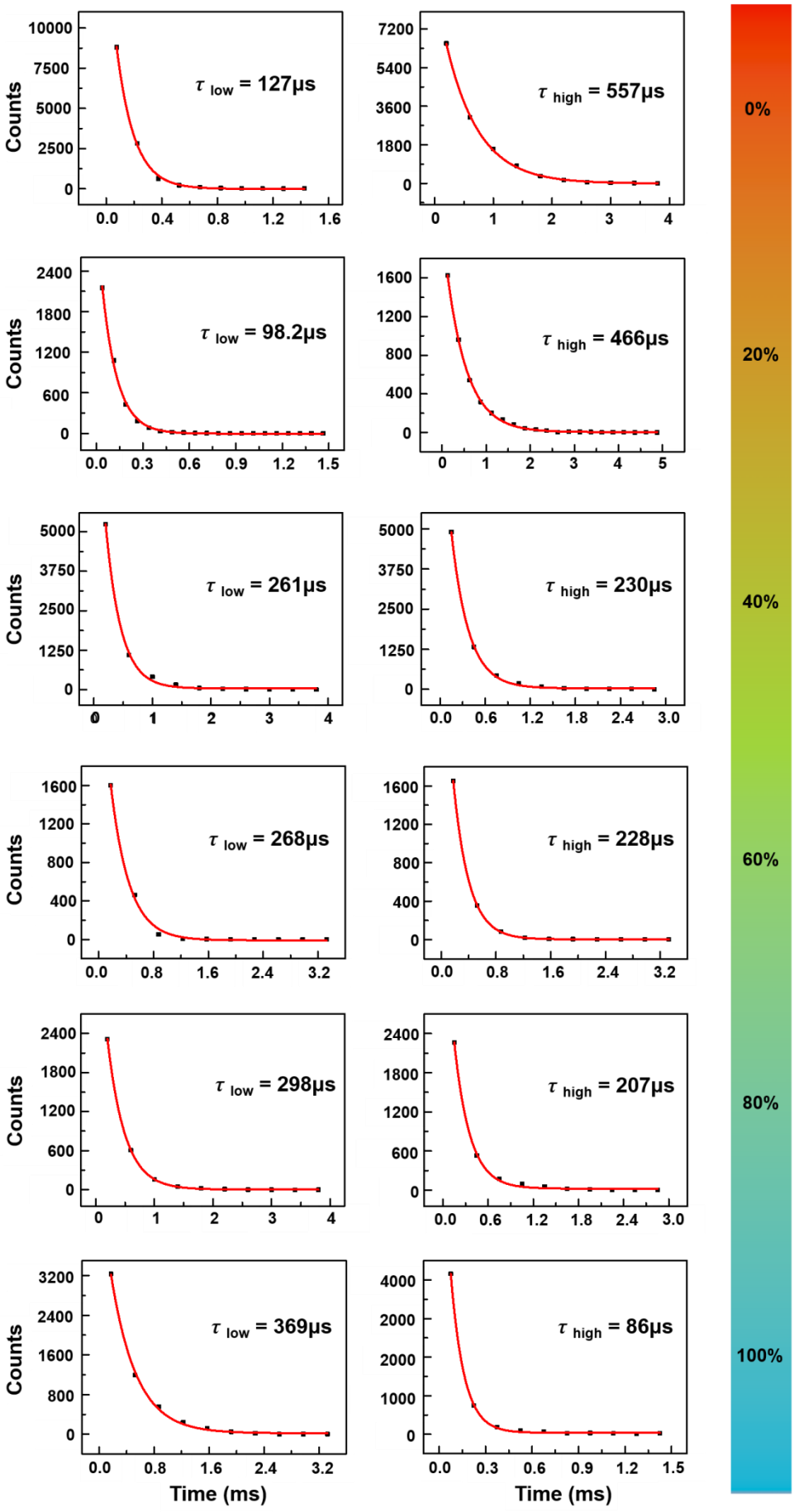
Counts
τ low = 127μs
τ high = 557μs
τ low = 98.2μs
τ high = 466μs
τ low = 261μs
τ high = 230μs
τ low = 268μs
τ high = 228μs
τ low = 298μs
τ high = 207μs
τ low = 369μs
τ high = 86μs
Time (ms)
Time (ms)
0%
20%
40%
60%
80%
100%

fig. S9. Plots of time intervals. Low (left) and high (right) current states in the idealized fit in Figure 3 for the single-molecule junction in the reaction solutions with 0% (a), 20% (b), 40% (c), 60% (d), 80% (e) and 100% (f) water as solvent, and single-exponential fittings derive the lifetimes of each state (τ_{low} and τ_{high}).

9. Additional solvent-dependent experiments

Under the same conditions, different proportions of cyclohexane were added into ethanol to reduce the polarity of solvents.

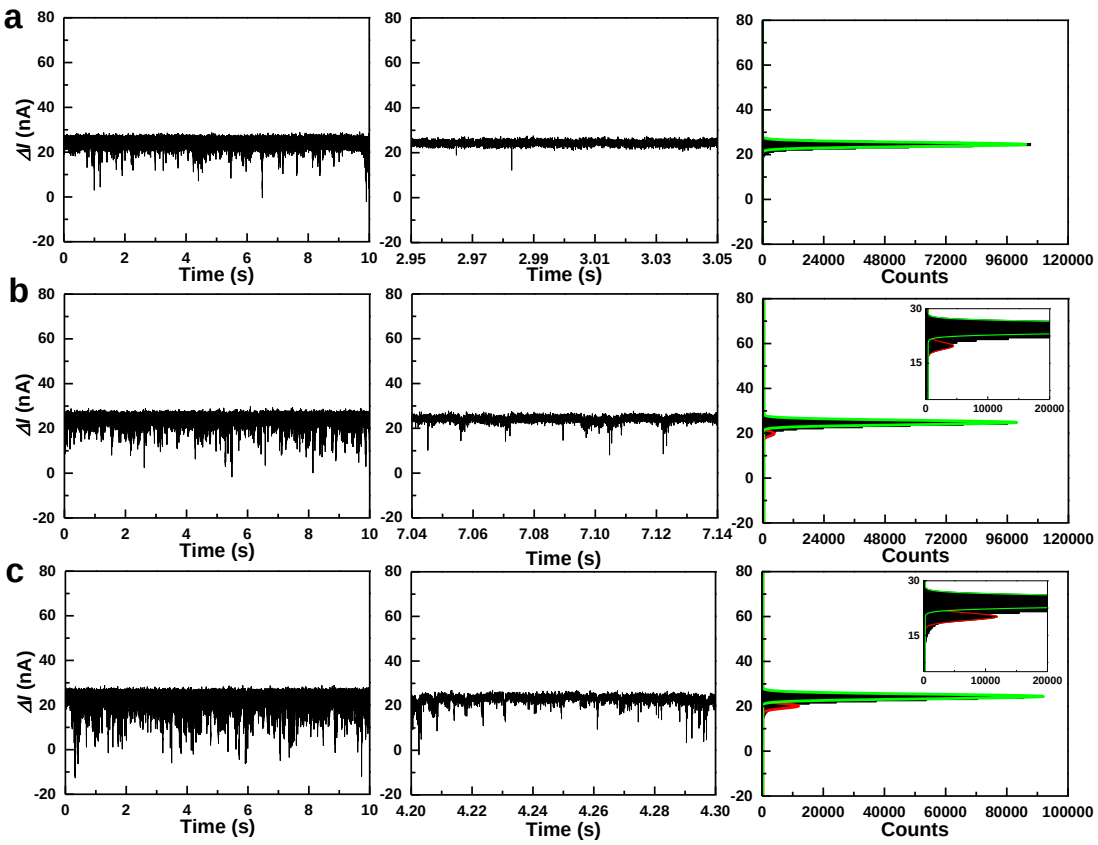

fig. S10. Additional solvent-dependent experiments. *I-t* curves and corresponding histograms of current values for a typical GMG-SMJ in the reaction solutions with 75% (**a**), 50% (**b**) and 25% (**c**) cyclohexane in ethanol at 298 K. V_D = 300 mV.